Appendix: Supplementary text 1

Center-specific definitions of amnestic mild cognitive impairment (aMCI) and subcortical vascular MCI (svMCI)

aMCI patients all met Petersen's criteria for MCI with these modifications [1]: (1) subjective memory complaint by the patient or his/her caregiver; (2) normal general cognitive function above the 16th percentile on the Korean Mini-Mental State Examination (MMSE); (3) normal activities of daily living as judged by both an interview with a clinician and the standardized activities of daily living (ADL) scale previously described; (4) objective memory decline below the 16th percentile on neuropsychological tests; and (5) not demented. In addition, we ensured that patients had minimal white matter hyperintensity (WMH) on magnetic resonance imaging (MRI): periventricular WMH [PWMH] <5 mm and deep WMH [DWMH] $<$ 10 mm in maximum diameter.

svMCI patients met the following modified Petersen's criteria [1]: (1) subjective cognitive complaint by the patient or his/her caregiver; (2) normal general cognitive function above the 16th percentile on the Korean MMSE; (3) normal activities of daily living as judged by both an interview with a clinician and the standardized ADL scale previously described; (4) objective cognitive decline below the 16th percentile on neuropsychological tests; and (5) not demented. Additionally, all svMCI patients had focal neurological symptoms or signs and significant ischemic changes on MRI. Focal neurological symptoms and signs included corticobulbar signs (facial palsy, dysarthria, dysphagia, or pathologic laughing or crying), pyramidal signs (hemiparesis, hyperactive deep tendon reflexes, or extensor plantar responses), or Parkinsonism (short-step gait, festination, shuffling gait, decreased arm swing while walking, rigidity, bradykinesia, or postural instability). The presence of significant ischemic changes associated with small-vessel disease was defined as WMH on MRI: PWMH (caps and rim) longer than 10 mm and DWMH $\geq$ 25 mm in maximum diameter. When defining DWMH, WMH located within the four axial slices just above the top of the lateral ventricles were considered to be PWMH, whereas WMH in the fifth or higher axial slices above the top of the lateral ventricle were considered to be DWMH. These imaging criteria indicate that our svMCI patients had ischemia sufficiently significant to meet at least grade 3 of Fazekas' ischemia criteria [2].

Supplementary text 2

Calculation of global Pittsburgh compound B (PiB) retention ratio

PiB-PET (positron emission tomography) images were co-registered to individual MRIs, which were normalized to a T_1-weighted MRI template. Using these parameters, MRI co-registered PiB-PET images were normalized to the MRI template. The quantitative regional values of PiB retention on the spatially normalized PiB images were obtained by automated VOIs analysis using an automated anatomical labeling (AAL) atlas. Data processing was performed using SPM Version 5 (SPM5) within Matlab 6.5 (MathWorks, Natick, MA).

To measure PiB retention, the cerebral cortical region to cerebellum uptake ratio (UR) was used. The cerebellum was used as a reference region as it did not show group differences. We selected 28 cortical volumes of interest (VOIs) from left to right hemispheres using the AAL atlas. The cerebral cortical VOIs chosen for this study were the bilateral frontal (superior and middle frontal gyri; medial portion of the superior frontal gyrus; opercular portion of the inferior frontal gyrus; triangular portion of the inferior frontal gyrus; supplementary motor area; orbital portion of the superior, middle, and inferior orbital frontal gyri; rectus and olfactory cortex), posterior cingulate gyri, parietal (superior and inferior, supramarginal and angular gyri, and precuneus), lateral temporal (superior, middle, and inferior temporal gyri, and heschl gyri), and occipital (superior, middle, and inferior occipital gyri, cuneus, calcarine fissure, and lingual, and fusiform gyri). Regional cerebral cortical URs were calculated by dividing each cortical VOI's UR by the mean uptake of the cerebellar cortex (cerebellum crus1 and crus2). Global PiB UR was calculated from the volume-weighted average UR of 28 bilateral cerebral cortical VOIs. We defined PiB UR as a continuous variable. Patients were considered PiB positive if their global PiB UR was more than two standard deviations (PiB retention ratio >1.5) from the mean of the normal controls.

Supplementary text 3

Imaging parameters for MRI acquisition

We acquired three-dimensional (3D) T1 turbo field echo MR images with the following imaging parameters: sagittal slice thickness, 1.0 mm, over contiguous slices with 50% overlap; no gap; repetition time (TR) of 9.9 ms; echo time (TE) of 4.6 ms; flip angle of 8°; and matrix size of 240 $\times$ 240 pixels, reconstructed to 480 $\times$ 480 over a field of view of 240 mm. The following parameters were used for the 3D fluid-attenuated inversion recovery (FLAIR) images: axial slice thickness of 2 mm; no gap; TR of 11,000 ms; TE of 125 ms; flip angle of 90°; and matrix size of 512 $\times$ 512 pixels.

Supplementary text 4

Image processing for cortical thickness measurement

Native MRI images were linearly transformed and registered into a standardized stereotaxic space [3]. The N3 algorithm was used to correct images for intensity-based nonuniformities [4] caused by nonhomogeneities in the magnetic field. Then, the registered and corrected images were classified into white matter, gray matter, cerebrospinal fluid, and background using a 3D stereotaxic brain mask and

the Intensity-Normalized Stereotaxic Environment for Classification of Tissues algorithm [5]. The surfaces of the inner and outer cortices were automatically extracted using the Constrained Laplacian-Based Automated Segmentation with Proximities algorithm [6].

Because of limitations in linear stereotaxic normalization, cortical thickness was calculated in native space rather than Talairach space. As we transformed MR volumes in native space into stereotaxic space with a linear transformation matrix, the inverse transformation matrix was applied to cortical thickness models to reconstruct them in native space [7]. Cortical thickness was defined as the Euclidean distance between linked vertices of inner and outer surfaces [6]. Thickness value was spatially normalized using surface-based two-dimensional registration with a sphere-to-sphere warping algorithm. Thus, vertices of each subject were nonlinearly registered to a standard surface template [8,9]. Cortical thickness was subsequently smoothed using a surface-based diffusion kernel to increase signal-to-noise ratio. We chose a kernel size of 20-mm full-width at half-maximum to maximize statistical power while minimizing false positives [10]. For global and lobar regional analyses, the data of 30 normal subjects who had previously been manually categorized to lobes with high inter-rater reliability [11] were registered to the template. The template then used the label of maximum probability in each vertex.

The presence of extensive WMH in MRI scans made it difficult to completely delineate the inner cortical surface with the correct topology due to tissue classification errors. To overcome this technical limitation, we automatically defined the WMH region using a FLAIR image and substituted it for the intensity of peripheral, normal-appearing tissue on the high-resolution T1 image after affine co-registration, as described in an earlier study [12].

Supplementary text 5

Image processing for hippocampal shape and volume measurement

Hippocampal shape analysis was based on boundary surfaces rather than volume measurement. Surface-based shape analysis and volume measurement have several advantages compared with volume-based approaches [13,14]. Thus, the boundary surfaces of the hippocampi were used to measure hippocampal volume, instead of voxel number. T1 images were processed to perform anatomical parcellations of each subject's hippocampus using the FreeSurfer software package (Version 5.0; Athinoula A. Martinos Center at Massachusetts General Hospital, Harvard Medical School; surfer.nmr.mgh.harvard.edu/). Labeled images with parcellation were transformed into the native anatomical space of the input MRI data. Subcortical mesh surfaces were then extracted from the labeled images for each subject using a Laplacian-based surface modeling system [15]. Next, every surface mesh from the population was registered to the mean surface mesh, which was used as a template mesh [16]. This surface registration provided vertex correspondences for hippocampal surface meshes. Thus, relative deformation of the hippocampal surface meshes against the template was calculated for each vertex. Based on this deformation data, subcortical surface volume was measured employing an algorithm proposed in a previous study [17].

Supplementary text 6

Neuropsychological tests and the calculation of composite scores for frontal and memory function

All patients underwent a standardized neuropsychological battery called the Seoul Neuropsychological Screening Battery (SNSB) [18]. This battery contains tests evaluating attention, language, praxis, four elements of Gerstmann syndrome, visuospatial processing, verbal and visual memory, and frontal/executive function. These included digit span forward/backward, Korean version of the Boston Naming Test, Rey-Osterrieth Complex Figure Test (copying, immediate and 20-min delayed recall, and recognition), the Seoul Verbal Learning Test (three learning-free recall trials of 12 words, 20-min delayed recall trial for these 12 items, and a recognition test), phonemic and semantic Controlled Oral Word Association Test (COWAT), the Stroop Test (word and color reading of 112 items during a 2-min period), the Mini-Mental State Examination, and Clinical Dementia Rating Sum of Boxes.

Using results from the SNSB, memory and frontal/executive subdomain scores were calculated as described in a previous study [19]. Memory-domain SNSB-D score (memory subscore) was calculated by summing scores of orientation, verbal memory, and visual memory tests. Memory subscores ranged from 0 to 150. Frontal/executive-domain SNSB-D score (frontal subscore) was calculated by summing scores from a category word generation task (COWAT for animal), a phonemic word generation task (phonemic COWAT), and Stroop color reading test. The frontal subscores ranged from 0 to 55.

Supplementary Table 1
Effects of predictors (PiB retention ratio, WMH volume, and the number of lacunae) on memory score through mean temporal-parietal thickness

	Mean temporal-parietal thickness			Memory score		
	β	SE	*P* value	β	SE	*P* value
Global PiB retention ratio	−0.070	0.025	.015	−13.536	2.413	.010
WMH volume	−0.002	0.001	.024	−0.078	0.093	.435
Lacunae	−0.001	0.001	.341	−0.333	0.139	.040
Mean temporal-parietal thickness				41.986	6.369	.010

Abbreviations: β, unstandardized beta coefficient; PiB, Pittsburgh compound B; SE, standard error; WMH, white matter hyperintensities.

NOTE. Values shown are the results of path analyses.

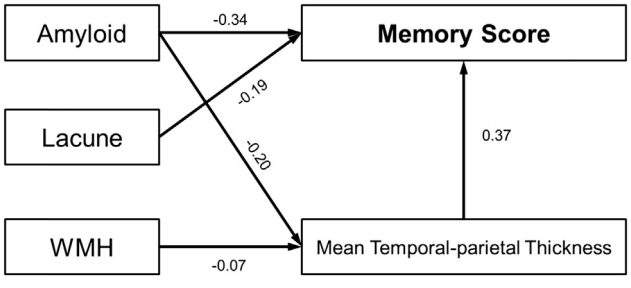

Supplementary Fig. 1. Schematic diagram of additional path analysis for memory score. Results of path analysis for memory function score. Mean temporal-parietal thickness was entered as a mediator variable. Amyloid burden, white matter hyperintensities (WMH), and the number of lacunae were entered as predictors. Age, gender, education, intracranial volume, and clinical group were entered as covariates. Numbers on the paths are standardized beta coefficients. Statistically significant direct paths were expressed. Abbreviations: SNSBD, Seoul Neuropsychological Screening Battery Domain.

References

[1] Seo SW, Cho SS, Park A, Chin J, Na DL. Subcortical vascular versus amnestic mild cognitive impairment: comparison of cerebral glucose metabolism. J Neuroimaging 2009;19:213–9.
[2] Fazekas F, Chawluk JB, Alavi A, Hurtig HI, Zimmerman RA. MR signal abnormalities at 1.5 T in Alzheimer's dementia and normal aging. AJR Am J Roentgenol 1987;149:351–6.
[3] Collins DL, Neelin P, Peters TM, Evans AC. Automatic 3D intersubject registration of MR volumetric data in standardized Talairach space. J Comput Assist Tomogr 1994;18:192–205.
[4] Sled JG, Zijdenbos AP, Evans AC. A nonparametric method for automatic correction of intensity nonuniformity in MRI data. IEEE Trans Med Imaging 1998;17:87–97.
[5] Zijdenbos A, Evans A, Riahi F, Sled J, Chui J, Kollokian V. Visualization in biomedical computing.
[6] Kim JS, Singh V, Lee JK, Lerch J, Ad-Dab'bagh Y, MacDonald D, et al. Automated 3-D extraction and evaluation of the inner and outer cortical surfaces using a Laplacian map and partial volume effect classification. Neuroimage 2005;27:210–21.
[7] Im K, Lee JM, Lee J, Shin YW, Kim IY, Kwon JS, et al. Gender difference analysis of cortical thickness in healthy young adults with surface-based methods. Neuroimage 2006;31:31–8.
[8] Lyttelton O, Boucher M, Robbins S, Evans A. An unbiased iterative group registration template for cortical surface analysis. Neuroimage 2007;34:1535–44.
[9] Robbins S, Evans AC, Collins DL, Whitesides S. Tuning and comparing spatial normalization methods. Med Image Anal 2004;8:311–23.
[10] Chung MK, Worsley KJ, Robbins S, Paus T, Taylor J, Giedd JN, et al. Deformation-based surface morphometry applied to gray matter deformation. Neuroimage 2003;18:198–213.
[11] Romero-Corral A, Montori VM, Somers VK, Korinek J, Thomas RJ, Allison TG, et al. Association of bodyweight with total mortality and with cardiovascular events in coronary artery disease: a systematic review of cohort studies. Lancet 2006;368:666–78.
[12] Jeon S, Yoon U, Park J-S, Seo SW, Kim J-H, Kim ST, et al. Fully automated pipeline for quantification and localization of white matter hyperintensity in brain magnetic resonance image. Int J Imaging Syst Technol 2011;21:193–200.
[13] Thompson PM, Hayashi KM, De Zubicaray GI, Janke AL, Rose SE, Semple J, et al. Mapping hippocampal and ventricular change in Alzheimer disease. Neuroimage 2004;22:1754–66.
[14] Wang L, Miller JP, Gado MH, McKeel DW, Rothermich M, Miller MI, et al. Abnormalities of hippocampal surface structure in very mild dementia of the Alzheimer type. Neuroimage 2006;30:52–60.
[15] Kim J, Park J. Organ shape modeling based on the Laplacian deformation framework for surface-based morphometry studies. J Comput Sci Eng 2012;6:219–26.
[16] Cho Y, Seong JK, Shin SY, Jeong Y, Kim JH, Qiu A, et al. A multi-resolution scheme for distortion-minimizing mapping between human subcortical structures based on geodesic construction on Riemannian manifolds. Neuroimage 2011;57:1376–92.
[17] Alyassin AM, Lancaster JL, Downs JH 3rd, Fox PT. Evaluation of new algorithms for the interactive measurement of surface area and volume. Med Phys 1994;21:741–52.
[18] Kang Y, Na DL. Seoul Neuropsychological Screening Battery: professional manual. Seoul: Human Brain Research & Consulting Co.; 2003.
[19] Ahn HJ, Chin J, Park A, Lee BH, Suh MK, Seo SW, et al. Seoul Neuropsychological Screening Battery-dementia version (SNSB-D): a useful tool for assessing and monitoring cognitive impairments in dementia patients. J Korean Med Sci 2010;25:1071–6.